Exp Oncol 2007
29, 2, 85–93

ORIGINAL CONTRIBUTIONS

Experimental ONCOLOGY

PLASMID ENCODING MATRIX PROTEIN OF VESICULAR STOMATITIS VIRUSES AS AN ANTITUMOR AGENT INHIBITING RAT GLIOMA GROWTH *IN SITU*

*H. Zhang[1, 2, #], Y.-J. Wen[1, #], B.-Y. Mao[2], Q.-Y. Gong[3], Z.-Y. Qian[1], Y.-Q. Wei[1, *]*

[1]*State Key Laboratory of Biotherapy for Human Diseases, West China Hospital, West China Medical School, Sichuan University, Chengdu, Sichuan, PR. China*

[2]*Department of Neurosurgery, West China Hospital, West China Medical School, Sichuan University, Chengdu, Sichuan, PR. China.*

[3]*Department of Radiology, West China Hospital, West China Medical School, Sichuan University, Chengdu, Sichuan, PR. China*

Aim: **Oncolytic effect of vesicular stomatitis virus (VSV) has been proved previously. Aim of the study is to investigate glioma inhibition effect of Matrix (M) protein of VSV *in situ*. *Materials and Methods:* A recombinant plasmid encoding VSV M protein (PM) was genetically engineered, and then transfected into cultured C6 gliomas cells *in vitro*. C6 transfected with Liposome-encapsulated PM (LEPM) was implanted intracranially for tumorigenicity study. In treatment experiment, rats were sequentially established intracranial gliomas with wild-typed C6 cells, and accepted LEPM injection intravenously. Possible mechanism of M protein was studied by using Hoechst staining, PI-stained flow cytometric analysis, TUNEL staining and CD31 staining. *Results:* M protein can induce generous gliomas lysis *in vitro*. None of the rats implanted with LEPM-treated cells developed any significant tumors, whereas all rats in control group developed tumors. In treatment experiment, smaller tumor volume and prolonged survival time was found in the LEPM-treated group. Histological studies revealed that possible mechanism were apoptosis and anti-angiogenesis. *Conclusion:* VSV-M protein can inhibit gliomas growth *in vitro* and *in situ*, which indicates such a potential novel biotherapeutic strategy for glioma treatment.**

Key Words: **gene therapy, glioma, liposome, matrix protein, plasmid, tumorigenicity, vesicular stomatitis virus.**

Malignant brain tumors constitute one of the most devastating forms of human cancer. More than 40% of all primary brain tumors arise from transformed glial cells and are thus classified as gliomas [1]. Despite advances in conventional therapy of gliomas over the past four decades [2], the prognoses of gliomas remain poor with median survival time of 15–28 months in stage III glioma (5-years survival rate of 30%), and that of 8–12 months in stage IV glioma (5-years survival rate of 2.5–5%) [3, 4]. The disappointing prognosis inspires the ongoing development of novel anti-glioma agents, which include gene therapy, immunomodulatory therapy and oncolytic viruses.

The potential of innovative gene transfer for glioma has been realized in several strategies. A subtopic of this field is represented by oncolytic virus, which is replication-competent and induces tumor cell lysis. Vesicular stomatitis virus (VSV), one of an important oncolytic virus, is an enveloped, negative-strand RNA virus and belongs to the family of *Rhabdoviridae*. It has been shown to replicate rapidly *in vitro* and kills a variety of tumor cell lines. The antitumor activity has been confirmed in both human tumor xenografts in nude mice and syngeneic tumors in the immunocompetent mice [5, 6]. Another experiment elucidated that VSV is furthermore effective on interferon non-responsive tumors [7]. Specially, VSV was proved to be an effective oncolytic agent in treatment of gliomas [8, 9]. VSV cell cytopathic effect includes inhibition of host gene expression, blockage of nucleocytoplasmic transport, and disruption of the host cytoskeleton, which results in rounding of infected cells [10]. According to these studies, VSV is an attractive candidate to be an oncolytic virus for glioma therapy. However, some evidence shows that VSV may cause fatal meningoencephalitis in experimental animals [11, 12]. Its clinical application should be considered conservatively due to possible toxic effects of live virus.

VSV has a major structural protein, the matrix (M) protein. The M protein plays a major role in the inhibition of host gene expression and induction of cell rounding that characterize VSV-infected cells. Expression of M protein in the absence of other viral proteins causes many cellular effects similar as infection with VSV by inhibition transcription of all three host RNA polymerases [13]. Based on these studies, we amplified the VSV M gene and cloned it into a eukaryotic plasmid as a novel agent for gene therapy. The antitumor effect of this agent was validated in rat C6 cells *in vitro* and intracranial glioma rat models *in vivo*.

MATERIALS AND METHODS

Plasmid construction. cDNA encoding VSV M protein was amplified from total RNA that were extracted from VSV-infected BHK21 cells by PCR (upstream primer 5'-CGC GGA TCC ATC ATG AGT TCC TTA AAG

Received: February 19, 2007.

#These authors contributed equally to this work.

*Corresponence: E-mail: yuquan.wei@hotmail.com

Abbreviations used: CTRL – control; DMSO – dimethyl sulfoxide; DOPE – dioleylphosphatidyl-ethanolamine; Gd-BOPTA – gadobenate dimeglumine; H&E – hematoxylin and eosin; M protein – matrix protein; MR – magnetic resonance; LEEP – liposome-encapsulated empty plasmid DNA; LEPM – liposome-encapsulated plasmid DNA encoding M protein; PI – propidium iodide; TUNEL – terminal deoxynucleotidyltransferase-mediated nick end labeling; VSV – vesicular stomatitis virus.

AAG-3', and downstream primer 5'- CGG AAT TCT CAT TTG AAG TGG CTG ATA GAA TCC-3'). The PCR product was inserted into eukaryotic expression vector pcDNA3.1(+) (Invitrogen), and the recombinant plasmid was named pcDNA-M. All the pcDNA-M plasmid was purified by using Qiagen Endo-Free plasmid purification column as described previously [14].

Cationic liposomes preparation. Liposomes containing DOTAP (Sigma D6182) in a 1 : 1 molar ratio with DOPE Dioleylphosphatidyl-ethanolamine (Sigma P1223) were prepared by solubilizing the lipid in chloroform and methanol at a volume ratio of 3 : 1. The lipid mixture was then dried as a thin layer in a round-bottomed flask under a stream of N_2. Residual chloroform and methanol was removed under high vacuum. The resulting lipid film was hydrated in 5% dextrose, and sonicated until solubilized completely in a bath sonicator. The Liposomes was sequentially extruded through polycarbonate membranes to generate small unilaminar vesicles. The Liposomes reagents were stored at 4 °C before use.

Tumor cells and cell culture. C6 (from American Type Culture Collection), a glioma cell line transformed from rat brain glial cell, was grown in Ham's F12K medium (Sigma-Aldrich) with 2 mM L-glutamine adjusted to contain 1.5 g/L sodium bicarbonate supplemented with 15% (vol/vol) horse serum, 2.5% (vol/vol) fetal bovine serum, and 50 pg/ml gentamycin. The cells were grown at 37 °C in 5% CO_2.

Transfection in vitro and MTT colorimetric assay. pcDNA-M and the empty plasmid DNA were encapsulated into liposomes before use. Briefly, an appropriate amount of pcDNA-M or empty plasmid DNA was gently mixed with the liposome solution at a mass ratio of 1 : 5. Then the mixture was incubated at 37 °C for 1 h. C6 cells were plated at 2×10^3 cells/200 µl into 96-well plates. After 24 h, cells were transfected with 2 µg liposome-encapsulated plasmid DNA encoding M protein (LEPM) and then cultivated for 24–72 h. Simultaneously, C6 cells were transfected with 2 µg liposome-encapsulated empty plasmid DNA (LEEP) or left untreated as controls. Each well was supplemented with 50 µl MTT solution of 2 mg/ml in complete media and incubated at 37 °C for 4 h. The medium and MTT solution were then removed, and 150 µl of dimethyl sulfoxide (DMSO) was added to each well. Absorbance was read at 490 nm using a microplate reader. The average of data for 6 wells was used. The experiment was repeated 3 times. The cells merely treated by media was served as the indicator of 100% cell viability.

Hoechst staining. Apoptosis was determined by staining with Hoechst 33258 (1 µg/ml; Beyotime). C6 cells were seeded on sterile cover glasses placed in the 6-well plates. After cell was adhered, 6 µg of LEPM was added into each well and co-cultivated for 48 h. Then, cells were fixed, washed twice with PBS and stained with Hoechst 33258 staining solution according to the manufacturer's instructions. Stained nuclei were observed under a fluorescence microscope (BX51; Olympus, Japan). Nuclear fragmentation and chromatin clumping were identified as characteristics of apoptosis. For the control, the same staining procedures were performed on cells with LEEP transfection or on those untreated.

Flow cytometry analysis. Flow cytometry analysis was performed to identify sub-G1 cells/apoptotic cells and measure the percentage of sub-G1 cells after propidium iodide (PI, Sigma) staining in hypotonic buffer as described [15, 16]. Briefly, after LEPM transfection as described above, cells were suspended in 1 ml hypotonic fluorochrome solution containing 50 µg/ml PI in 0.1% sodium citrate plus 0.1% Triton X-100, and the cells were analyzed by using a flow cytometer (ESP Elite, Beckman Coulter, Fullerton, CA). Apoptotic cells appeared in the cell cycle distribution as those cells with DNA content less than that of G1 cells.

Tumor cells implantation. Six-week-old male Wistar rats (200 g) were used. All animals were maintained in a barrier facility. Experiments were approved by the Animal Research Committee of Sichuan University (Chengdu, Sichuan, P.R.China). The confluent C6 cells were trypsinized and re-suspended in DMEM free of serum immediately before implanting to host animals. The animals were anesthetized with a ketamine/xylazine mixture. The head was shaved, following which the skull was exposed. The animal was positioned into a stereotactic frame (David Kopf) with small animal earbars. A burr hole was made using a Dremel drill approximately 3 mm right lateral and 0.5 mm anterior from the intersection of the coronal and sagittal sutures (bregma). Cells (1×10^6) were injected using a 26-gauge, beveled-tip Hamilton syringe at a depth of 5 mm in a volume of 10 µl. The needle was left in place for 2 min after injection to limit leakage.

Tumorigenicity studies. To investigate the efficacy of M protein, the experiment of tumorigenicity was performed. LEPM was transfected into C6 tumor cells *in vitro*, then the transfected C6 cells were implanted intracranially into 5 Wistar rats. In control, C6 cells were transfected with LEEP and then implanted into another 5 Wistar rats.

Therapeutic studies. Wild-type C6 cells were implanted into 15 Wistar rats intracranially as described previously. When tumor volume reached about 60 mm^3 (after 10 days of cells implantation), 5 rats bearing intracranial gliomas were intravenously injected with 150 µg/200 µl of LEPM to explore the therapeutic effect of M protein. LEEP with corresponding dose was intravenously injected in another 5 rats of control group. Rats were treated for 6 times with an interval of 2 days. Additionally, the third group of 5 rats bearing gliomas was left untreated. These rats were monitored each day for neurological symptoms and for survival.

MR imaging methods. Experimental rats received magnetic resonance imaging (MR imaging) scan at day 10, 17, and 24 respectively after tumor cell implantations. The animals were anesthetized with a ketamine/xylazine mixture. 0.5-mmol/L solution of gadobenate dimeglumine (Gd-BOPTA) was injected in the tail vein at a dose of 0.1 mmol/kg. Serial T1-weighted spin-echo images were obtained 5 min after injection with a 3.0-T superconducting system (3.0T GEMSExct, GE Co.) using the following parameters: 514/28 (TR/TE); field of view, 4.5 cm; section

thickness, 1.6 mm; matrix, 64 × 64; averaging, two times. Tumor volumes estimated in all experimental animals were obtained by manual segmentation of MR imaging data that were corrected for interslice distances.

Histological and immunohistochemistry analysis. A duplicated therapeutic studies, as described previously, were performed for histological and immunohistochemistry analysis. Five rats in each group were sacrificed after 20 days of tumor cell implantation by overdose of ether. Whole brain was taken out carefully and then fixed in 4% (wt/vol) formaldehyde for 7 days. Paraffin tissue sections, 5 μm thick, were stained with hematoxylin and eosin (H & E). H & E section along the largest diameter of the tumor was scanned in the low field using computer aided image analysis system Quantimet 600 and Qwin software (Leica, Benshaim, Germany). For the observations of potential side effects on treated rats, the tissues of heart, liver, spleen, lung, kidney, brain were fixed in 4% formaldehyde, embedded in paraffin, and stained with H & E.

For immunohistochemistry analysis, paraffin tissue blocks were sectioned (5 μm) and dewaxed by three 5-min incubations in xylene, followed by 3 incubations in absolute ethanol. Endogenous peroxidases were blocked in 0.3% hydrogen peroxide for 30 min at room temperature, followed by antigen retrieval in 1 mM EDTA with microwave heating for 30 min. Prior to staining, all slides were washed in PBS and non-specific binding sites blocked by incubation with PBS containing 1% BSA. For detection of platelet endothelial cell adhesion molecule-1(CD31), sections were probed with a monoclonal mouse anti-rat CD31 antibody (1 : 400; Santa Cruz Biotechnology) at 41 °C overnight, followed by incubation with biotinylated polyclonal rabbit anti-mouse antibody (1 : 200; Vector, Burlingame, CA). Positive reaction was visualized using 3,3-diaminobenzidine as chromagen (DAB substrate kit; Vector). Sections were counterstained with hematoxylin and mounted with glass coverslips. To evaluate microvessel quantitation, 5 areas considered to have the highest densities in slices were selected and counted at × 400 power magnification, and mean values ± SEM were recorded. Any brown-staining endothelial cell or cluster of endothelial cells with or without a lumen, clearly separated from adjacent microvessels, tumor cells, and other connective tissue elements, was considered to be individual vessels. All counts were performed by two investigators in a blinded manner.

Detecting of apoptosis by TUNEL assay. Fluorescent *in situ* terminal deoxynucleotidyltransferase-mediated nick end labeling (TUNEL) assay was performed using an *in situ* apoptotic cell detection kit (Boehringer Mannheim, Indianapolis, IN) following the manufacturer's protocol. It was based on the enzymatic addition of digoxigenin nucleotide to the nicked DNA by terminal deoxynucleotidyl transferase. Images were captured by fluorescence microscope at × 400 magnification (Olympus). The apoptosis were quantitated by counting TUNEL positive cells from three areas in each section in a blinded manner.

Statistical analysis. Experiment data were reported as mean ± SD. Survival analysis was conducted to determine if LEPM injection benefited animals and computed by the Kaplan-Meier method and tested by Log Rank method. Statistical analysis of tumor volume was performed by One-way ANOVA. Statistical significance was determined at the level of $P \leqslant 0.05$.

RESULTS

Induction of apoptosis by M protein in vitro. The biological activity of VSV M protein was tested against cultivated C6 glioma cells by transient transfection with complex of liposome and VSV-M plasmid. Apparently, growth of C6 cells of LEPM group was inhibited, compared with LEEP or non-transfected control groups. (Fig. 1, *a*, *b*, *c*). Cell viability was also determined by MTT assay. As shown in Fig. 1, *d*, the viabilities of cells treated with LEPM were 73% at 48 h and 45% at 72 h respectively, and the viabilities of cells treated by LEEP were similar to the untreated group.

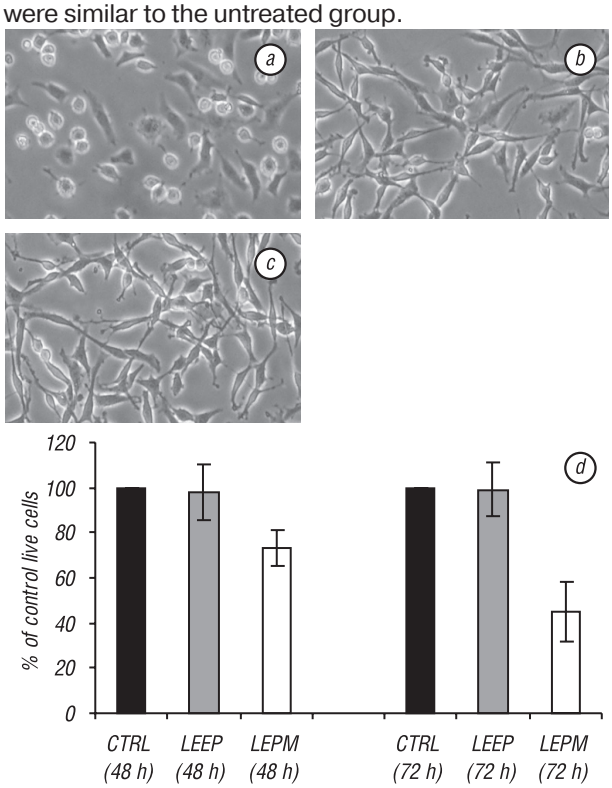

Fig. 1. Induction of cytopathy on C6 glioma cells *in vitro* with the treatment of LEPM. C6 cells were treated with LEPM (*a*) for 72 h. As controls, C6 cells were treated with LEEP (*b*) or left untreated (*c*). Phase-contrast micrographs of monolayer were recorded. M protein showed apparent cytopathic effect on glioma cells compared with controls. Viability of cells was also calculated by MTT assay (*d*). C6 cells were treated with LEPM (blank bar), while LEEP (gray bar) and left untreated (black bar) as controls. Results of MTT were shown as mean ± SD of 6 wells and triplicate experiments. In each experiment, the media-only treatment (left untreated) indicated 100% cell viability

Hoechst staining was performed to identify the type of cell death induced by M protein. The apoptosis of C6 glioma cells after treatment of M protein for 48 h was detected. The increase of number of these cells was more significant in treatment group than the control. Fewer apoptotic changes were detected in C6 cells that were treated with LEEP or left untreated (Fig. 2).

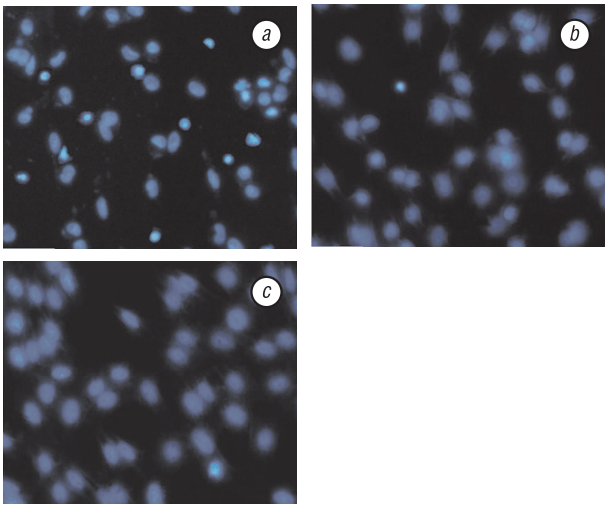

Fig. 2. C6 cells were incubated with or without LEPM. The nuclei of the corresponding cells were demonstrated by blue Hoechst 33258 staining. Apoptotic cells with nuclear fragmentation and chromatin clumping are evident after treatment of LEPM (*a*) while apoptotic changes were not detected in C6 cells treated by LEEP (*b*) or left untreated (*c*). Magnification for images was × 400

C6 cells transfected with LEPM, LEEP or un-transfected were stained with PI and analyzed by flow cytometry for further confirmation (Fig. 3). The sub-G1 cells of LEPM group accounted for 36.9%, while LEEP group and untreated group accounted for 6.5% and 5.4% respectively.

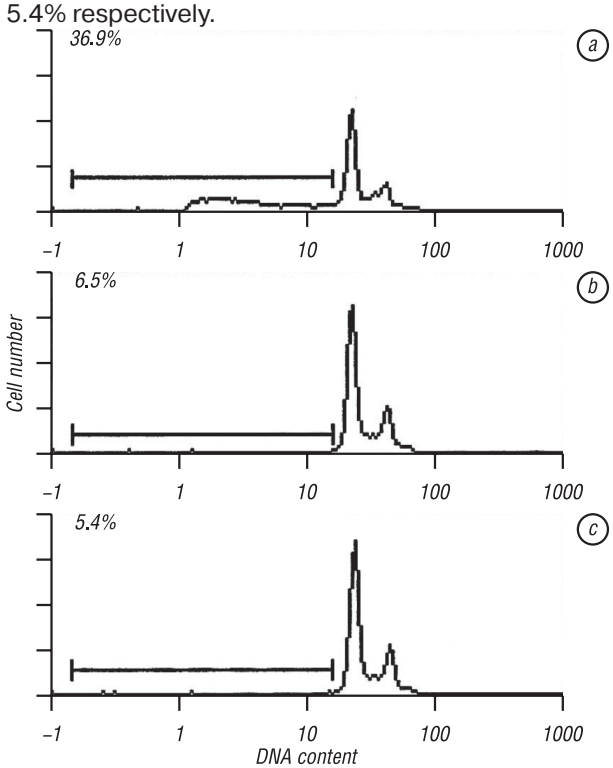

Fig. 3. Flow cytometry analysis of PI stained cells 48 h after transfection. Percentage of sub-G1/apoptotic C6 cells treated by LEPM (6 μg) for 48 h accounted for 36.9% (*a*). Correspondingly, the LEEP group and the untreated group accounted for 6.5% (*b*) and 5.4% (*c*) respectively

Effect of LEPM or LEEP on tumorigenicity of gliomas. C6 glioma cells were transfected with LEPM or LEEP, and then injected intracerebrally into Wistar rats. All 5 animals of control group that were injected with LEEP-transfected C6 cells developed tumors, whereas none of the animals injected with LEPM developed any significant tumor by MR imaging (Fig. 4, *a*, *b*). The results were verified by two independent experiments.

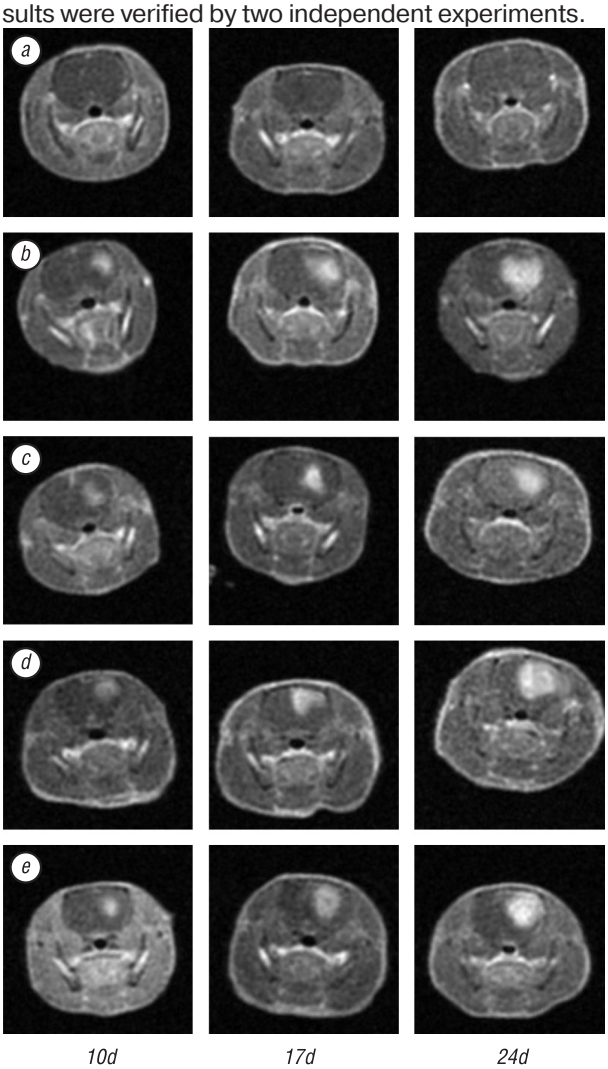

Fig. 4. MR imaging. Several Gd-enhanced T1-weighted MR images obtained 10 days, 17 days, and 24 days after implantation of C6 glioma cells respectively. No significant tumor was demonstrated by contrast enhancement at least in 24 days after LEPM-transfected tumor cells implantation (*a*). Conversely, the tumors of the control group implanted with LEEP-transfected tumor cells demonstrated strong contrast enhancement (*b*). In therapeutic studies, animals were implanted with wild type C6 gliomas (*c*–*e*). Tumor growth was inhibited after accepted LEPM treatment (*c*), comparing with LEEP mock group (*d*) and untreated control group (*e*)

Inhibition of established gliomas in vivo. Established intracranial gliomas were confirmed by MR images at day 10. The tumor appeared as expansive strongly contrast-enhancing lesions on T1-weighted sequences following injection of Gd-BOPTA (Fig. 4, *c*–*e*). All of 5 rats injected with LEPM showed slightly slower rate of tumor growth when checking on day 17 after implantation. And the growth rate of LEPM group decreased obviously on day 24. A review of MR images obtained at day 24 after cells implantation showed that the mean tumor volume in LEPM group was 182.4 ± 40.16 mm^3, 312.0 ± 56.15 mm^3 in LEEP group, and 296.0 ± 42.33 mm^3 in untreated group. Quantization of tumor volumes by MR imaging studies showed a significant volume reduction ($P = 0.004$) in LEPM group compared with that in untreated group at

day 24. Nevertheless, the difference between LEEP group and untreated group was not significant (P = 0.635) (Fig. 5, *a*).

Survival analysis showed that rats in LEPM group had prolonged survival time, which extended 11.4 days after treatment (37.2 ± 5.2 days vs 25.8 ± 3.0 days). (Fig. 5, *b*) These results indicated that M protein acts as a potential gliomas growth inhibitor.

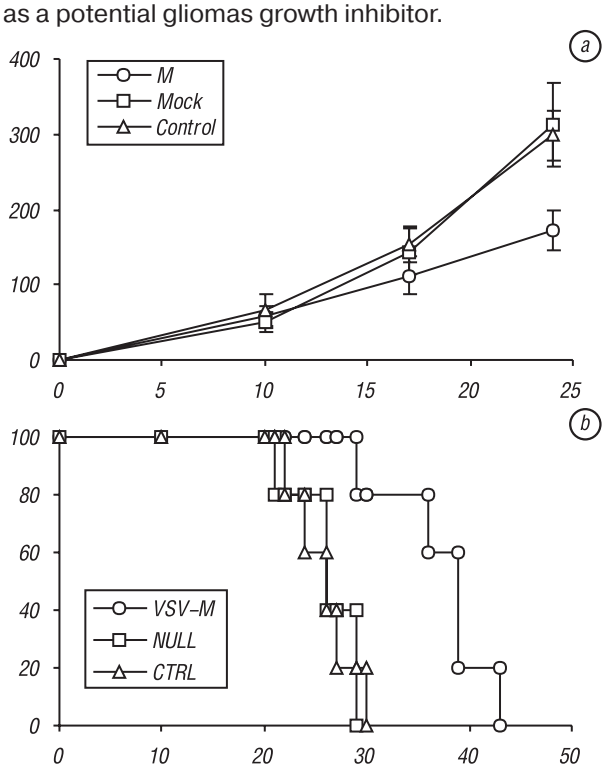

Fig. 5. Tumor volume and survival plot. *a* — Graphs showing assessments of tumor volumes (Mean ± SD) of each group. Rats bearing intracerebral gliomas were injected with LEPM (150 μg) intravenously starting at day 10 after C6 cells implantation. The LEEP group received treatment of intravenous injection of LEEP (150 μg), and the CTRL group was left untreated. The comparison of the three curves revealed VSV-M treatment inhibited growth of intracerebral tumors. The tumor volumes showed significant difference between VSV-M and control groups (172.8 ± 26.29 mm^3 vs 298.7 ± 33.3 mm^3 P = 0.002). While the difference between the LEEP group and control group was not significant (312.0 ± 56.15 mm^3 vs 298.7 ± 33.3 mm^3, P = 0.673). *b* — Kaplan-Meier survival curves of rats bearing C6 gliomas and subjected to the VSV-M plasmid treatment. Mean survival time of the LEPM group, LEEP group, and CTRL group were 37.2 ± 5.2 days, 26.2 ± 3.3 days, 25.8 ± 3.0 days respectively (P = 0.001). Differences between survival times of LEPM group and LEEP group (P = 0.0084), or CTRL group (P = 0.0064) were significant. There was no statistical difference between survival times of LEEP group and CTRL group (P = 0.9952). LEPM, *liposome-encapsulated plasmid encoding VSV-M protein treated group*; LEEP, *liposome-encapsulated empty plasmid treated group*; CTRL = *untreated control group*

Inhibition of tumor-induced angiogenesis and increasing apoptosis by LEPM and LEEP. Histopathological studies of tumor section by hematoxylin and eosin (H & E) staining after 20 days of implantation showed various amount of tumor cells with high nuclear/cytoplasmic ratio at the ipsilateral sites. In the process of tumor invasion, the tumor had replaced and destroyed the grey and white matter, in several instances, extended from the surface of the brain to the ventricles. At low magnification, the tumor appeared to have relatively well defined boundaries.

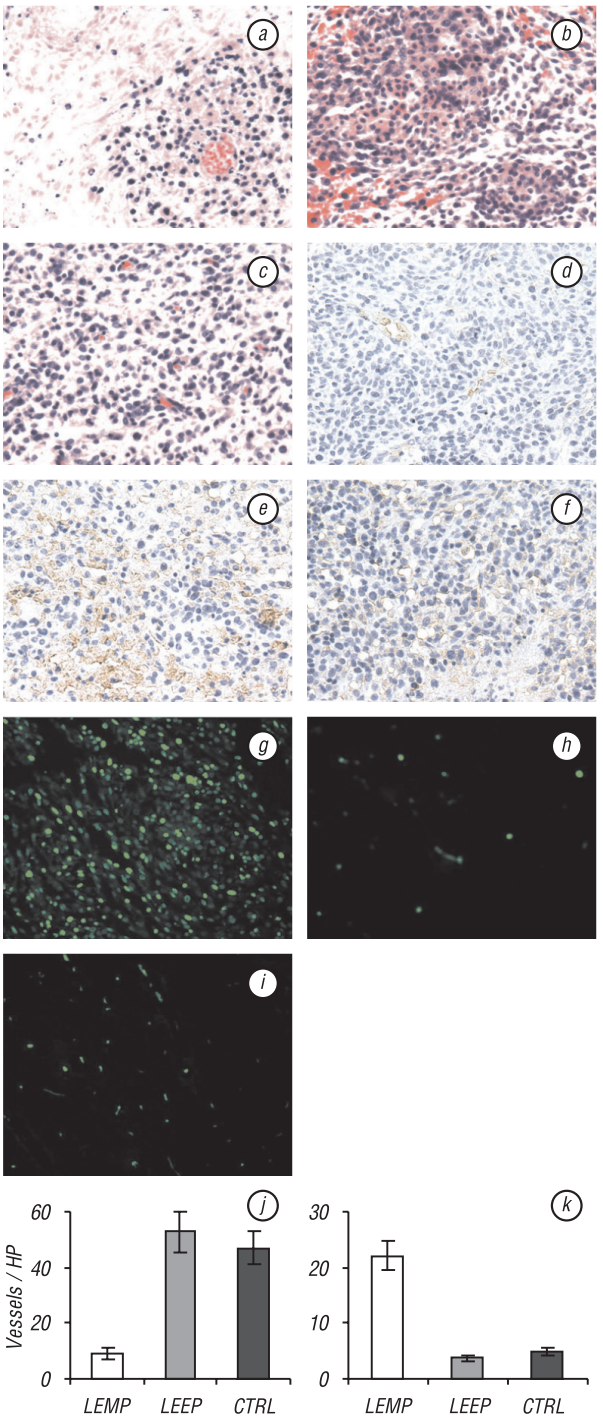

Fig. 6. Histological study and TUNEL staining. Representative histology section of a tumor-bearing animal treated with VSV-M plasmid (× 400). Extensive necrosis can be observed in the LEPM group *(a)* apparently more than LEEP group *(b)* and untreated control group *(c)*. Paraffin tissue section was treated with rat anti-CD31 antibody (× 400). Significantly decreased microvessels were observed in gliomas of the LEPM-treated group *(d)*. Massive microvessels were stained in gliomas of the LEEP-treated group *(e)* and the untreated control group *(f)*. Fluorescent in situ terminal deoxynucleotidyl transferase-mediated nick end labeling (TUNEL) assay was performed using an in situ apoptotic cell detection kit (Boehringer Mannheim, Indianapolis, IN) following the manufacturer's protocol at day 20 after implantation. Apoptotic nuclei (green) were observed under a fluorescence microscope (× 400). The treatment with LEPM *(g)* showed apparent apoptotic cells compared to treatment with LEEP treated group *(h)* and untreated control groups *(i)*. Vessel density *(j)* and apoptosis quantitation *(k)* of each group was determined by counting the number of microvessels or TUNEL positive cells per high-power field in each section

But at higher magnification, it was clear that fingers of tumor extended beyond the main mass into adjacent brain tissue, which often had a perivascular orientation (Fig. 6, *a–c*). More necrosis was detected in the tumor of LEPM group (Fig. 6, *a*). Viable glioma cells confounded with the necrotic areas. In contrast, extensive necrosis was seldom observed in the tumor of LEEP treated mock animals (Fig. 6, *b*) and untreated control animals (Fig. 6, *c*).

Immunohistochemistry studies of CD31 demonstrated a decreased microvessel density, counted from five different high-power fields, in 20-day tumor tissues obtained from the LEPM group (9.03 ± 1.79, Fig. 6, *d*, *j*) compared with control tumor tissues of LEEP group (52.71 ± 7.24, Fig. 6, *e*, *j*) and untreated CTRL group (47.09 ± 5.86, Fig. 6, *f*, *j*). The microvessel density was quantified by using five rats in each group.

Apoptosis-related molecular markers on tumor sections were examined to explore the role of apoptosis on tumor inhibition effect. TUNEL staining revealed apparently more apoptotic cells in tumors obtained from the LEPM group (22.13 ± 2.62%, Fig. 6, *g, k*), compared with control tissues of LEEP group (3.79 ± 0.53%, Fig. 6, *h*, *k*) and untreated CTRL group (4.88 ± 0.68%, Fig. 6, *i*, *k*).

DISCUSSION

Some conditionally replicating viruses can replicate in tumor cells and show great promise as antitumor agents for cancer therapy. These viruses can be genetically engineered for oncolytic purposes and denominated as oncolytic viruses [17, 18]. The viruses that have been modified for oncolysis are adenoviruses, HSV-1, and some RNA viruses such as Reovirus and Rhabdovirus [19, 20]. Vesicular stomatitis virus (VSV), the prototype of Rhabdoviridae family, Vesiculovirus genus, is a recent addition to the list of oncolytic viruses [21]. Vesicular stomatitis virus causes rapid induction of apoptosis and cell death [22–24]. Several researchers have demonstrated potential advantages of using VSV as an anticancer vector, highlighting not only its ability to kill cells that are interferon nonresponsive [25], but also its ability to kill cells that lack important tumor suppressors such as p53 or that are transformed by oncogenes such as *Ras* and *Myc* [26, 27]. Other studies have demonstrated that Infection of cells with VSV results in a rapid inhibition of cellular macromolecular synthesis shortly after infection and the development of a cytopathic effect (CPE) which is manifested starting about 4 h after infection by the rounding of cells [28, 29]. Studies with syngeneic cancer models have extended these findings, demonstrating effective tumor lysis in a system with an intact immune system [30].

Although oncolytic viruses have clinical potential as antitumor agents, evidence indicates that current versions of these viruses may have some limited therapeutic benefit. To begin with, wild-type oncolytic virus should be genetically engineered for viral replication only in tumor cells, rather than normal cells. Therefore, gene deletions that confer viral replication selectivity also frequently reduce the potency of virus in tumor [31]. Secondly, unlike other therapeutic strategies, the antitumor activity of oncolytic viruses does not induce a significant bystander effect, a process that can result in the killing of non-transduced cells after death of the transduced neighbouring cells. The bystander effect is considered to be crucial for effective antitumor therapy, because it compensates for the limited efficiency of vector delivery and spread [32, 33]. Furthermore, intravascular administration may deliver oncolytic viruses to tumors, but its efficiency is impeded by an antiviral activity of rodents and humans and requires suppression of innate and elicited antiviral responses [34]. Finally, the biological safety of replicate-capable viruses should be considered carefully. Specially, several independent researches have indicated that VSV may cause a fatal meningoencephalitis in experimentally infected mice [11, 12]. For all these reasons mentioned above, the oncolytic viruses have many limitations that may prevent them from entering the mainstream of clinical oncology [35].

To avoid these weaknesses, the matrix (M) protein of VSV was chosen to provide an alternative in anti-glioma therapy. VSV contains a single-stranded negative sense RNA genome which encodes five mRNAs that are translated into five proteins referred to as nucleocapsid (N), polymerase protein (P) and (L), surface glycoprotein (G), and a peripheral matrix protein (M) [36-38]. The M protein is primarily responsible for cytopathic effects associated with VSV infection. The M protein is initially a soluble cytoplasm protein, which binds to cellular membranes during the budding process. In addition, some findings suggest that activation of caspase-3 by VSV infection is required for efficient apoptosis induction [23]. It has been reported that the M protein is remarkable for a number of different roles in virus-infected cells, including its ability to inhibit host gene expression, to induce cell rounding and to induce apoptosis [39]. To investigate the effect of VSV matrix protein on tumor growth, we constructed a plasmid DNA encoding VSV M protein and observed its effect on gliomas *in vitro* and *in vivo*.

The study of tumorigenesis and evaluation of therapeutic effects require accurate and reproducible brain tumor animal models. Implantation models of glioma we chose could exhibit features of human disease states including glial differentiation of tumor cells, diffuse infiltration, microvascular proliferation, and resemble of progression kinetics and antitumor immune responses [40].

Additionally, we established a method for monitoring the growth of intracranial gliomas by using Gd-BOPTA-enhanced MR images. Enhanced MR imaging can provide real-time images of intracranial gliomas in physiological conditions [41, 42]. Additionally, we can calculate relatively precise tumor volumes by enhanced MR images for the purpose of comparing treatment effects among groups [43]. The tumor volume growth curves showed that when intracranial gliomas reached volume of about 300 mm^3, rats bearing tumors began to die. Meanwhile, the curves showed

that when untreated group and null-plasmid treated group reached death volumes after about 3 weeks of post-implantations, the VSV-M plasmid treated group was 172.8 ± 26.29 mm^3. Inhibition of tumor growth prolonged survival time for about 11 days.

To our knowledge, this is the first time when it was demonstrated that the VSV-M protein would induce glioma cytopathy *in vitro*, and inhibit the growth of established intracranial rat glioma *in situ*. The antitumor efficacy *in vitro* and *in situ* may result from increased induction of the apoptosis in treatment group. This suggestion is supported by the present findings. The glioma cells transfected with LEPM *in vitro* displayed obvious cytopathic effect observed by phase-contrast microscopy-apparent increase in the number of sub-G1 cells of PI-stained nuclei analyzed by flow cytometry. Morphologic changes of nuclei observed by Hoechst staining confirmed that the cell death was resulted from apoptosis. In addition, apoptotic cells in tumors treated with LEPM were more apparent in fluorescent *in situ* TUNEL assay compared with those in LEEP or untreated groups. The induction of apoptosis by wtVSV-M protein is dependent on activation of the intrinsic pathway, requiring activation of the initiator caspase, caspase-9 [44]. A primary function of wt M protein is to inhibit host gene expression which results in cellular stress that activates the mitochondrial apoptotic pathway.

Another possible mechanism of the anti-angiogenesis effect may account for tumor inhibition. It has been proved that the progression of solid tumors depends on angiogenesis [45]. Selective inhibition or destruction of the tumor vasculature could trigger tumor growth inhibition [46]. We observed microvessel decrease in LEPM group by CD31 staining and thought it may play some role in tumor inhibition, even though we did not know the exact mechanism and the relationship with tumor cells apoptosis.

CONCLUSION

We reported that Matrix (M) protein of vesicular stomatitis virus (VSV) can inhibit rat glioma growth either *in vitro* or *in situ*. We observed apparent tumor cells death after transfected with VSV-M plasmid along with decreased growth of intracranial gliomas and prolonged survival time after VSV-M plasmid injections. No matter *in vitro* or *in situ*, tumor cell apoptosis was apparently observed and thought to be the most important mechanism of tumor inhibition. Additionally, anti-angiogenesis phenomenon was surveyed at immunohistochemistry studies and thought to be another possible mechanism. The findings in the present study may provide a new biotherapeutic strategy for the treatment of gliomas. M protein is considered safer than live VSV, and easier for gene recombination. As a potent inhibitor of gliomas, M protein could play more important roles in glioma therapy such as binding some glioma-specific ligand to achieve targeting character [47, 48], and, when placed in the resection cavity at surgery, killing residual glioma cells [49].

ACKNOWLEDGEMENTS

This study was supported by Major State Basic Research Development Program of China (973 Program) (No 2004CB518807); National Natural Science Foundation Program of China (No. 30200339); Sichuan Application Foundation Research Program (No 04JY029-085-3).

REFERENCES

1. **Walker AE, Robins M, Weinfeld FD.** Epidemiology of brain tumors: the national survey of intracranial neoplasms. Neurology 1985; **35**: 219–26.

2. **Reardon DA, Rich JN, Friedman HS, Bigner DD.** Recent advances in the treatment of malignant astrocytoma. J Clin Oncol 2006; **24**: 1253–65.

3. **Decaestecker C, Salmon I, Camby I, Dewitte O, Pasteels JL, Brotchi J, Van Ham P, Kiss R.** Identification of high versus lower risk clinical subgroups in a group of adult patients with supratentorial anaplastic astrocytomas. J Neuropathol Exp Neurol 1995; **54**: 371–84.

4. **Scott CB, Nelson JS, Farnan NC, Curran WJ Jr, Murray KJ, Fischbach AJ, Gaspar LE, Nelson DF.** Central pathology review in clinical trials for patients with malignant glioma. A Report of Radiation Therapy Oncology Group 83-02. Cancer 1995; **76**: 307–13.

5. **Balachandran S, Porosnicu M, Barber GN.** Oncolytic activity of vesicular stomatitis virus is effective against tumors exhibiting aberrant p53, ras, or myc function and involves the induction of apoptosis. J Virol 2001; **75**: 3474–9.

6. **Ebert O, Shinozaki K, Huang T-G, Savontaus MJ, Garcia-Sastre A, Woo SLC.** Oncolytic vesicular stomatitis virus for treatment of orthotopic hepatocellular carcinoma in immune-competent rats. Cancer Res 2003; **63**: 3605–11.

7. **Stojdl DF, Lichty B, Knowles S, Marius R, Atkins H, Sonenberg N, Bell JC.** Exploiting tumor-specific defects in the interferon pathway with a previously unknown oncolytic virus. Nat Med 2000; **6**: 821–5.

8. **Duntsch CD, Zhou Q, Jayakar HR, Weimar JD, Robertson JH, Pfeffer LM, Wang L, Xiang Z, Whitt MA.** Recombinant vesicular stomatitis virus vectors as oncolytic agents in the treatment of high-grade gliomas in an organotypic brain tissue slice-glioma coculture model. J Neurosurg 2004; **100**: 1049–59.

9. **Wollmann G, Tattersall P, van den Pol AN.** Targeting human glioblastoma cells: comparison of nine viruses with oncolytic potential. J Virol 2005; **79**: 6005–22.

10. **Connor JH, Lyles DS.** Inhibition of host and viral translation during vesicular stomatitis virus infection. eIF2 is responsible for the inhibition of viral but not host translation. J Biol Chem 2005; **280**: 13512–9.

11. **Cornish TE, Stallknecht DE, Brown CC, Seal BS, Howerth EW.** Pathogenesis of experimental vesicular stomatitis virus (New Jersey serotype) infection in the deer mouse (Peromyscus maniculatus). Vet Pathol 2001; **38**: 396–406.

12. **Huneycutt BS, Plakhov IV, Shusterman Z, Bartido SM, Huang A, Reiss CS, Aoki C.** Distribution of vesicular stomatitis virus proteins in the brains of BALB/c mice following intranasal inoculation: an immunohistochemical analysis. Brain Res 1994; **635**: 81–95.

13. **Kopecky SA, Lyles DS.** Contrasting effects of matrix protein on apoptosis in HeLa and BHK cells infected with vesicular stomatitis virus are due to inhibition of host gene expression. J Virol 2003; **77**: 4658–69.

14. **Timares L, Safer KM, Qu B, Takashima A, Johnston SA.** Drug-inducible, dendritic cell-based genetic immunization. J Immunol 2003; **170**: 5483–90.

15. **Gorczyca W, Gong J, Ardelt B, Traganos F, Darzynkiewicz Z.** The cell cycle related differences in susceptibility of HL-60 cells to apoptosis induced by various antitumor agents. Cancer Res 1993; **53**: 3186–92.

16. **Barry MA, Reynolds JE, Eastman A.** Etoposide-induced apoptosis in human HL-60 cells is associated with intracellular acidification. Cancer Res 1993; **53** (Suppl): 2349–57.

17. **Chase M, Chung RY, Chiocca EA.** An oncolytic viral mutant that delivers the CYP2B1 transgene and augments cyclophosphamide chemotherapy. Nat Biotechnol 1998; **16**: 444–8.

18. **Rampling R.** Oncolytic virus therapy for brain tumours. Br J Cancer 2003; **88** (Suppl): S6–6.

19. **Mathis JM, Stoff-Khalili MA, Curiel DT.** Oncolytic adenoviruses — selective retargeting to tumor cells. Oncogene 2005; **24**: 7775–91.

20. **Nakamori M, Fu X, Meng F, Jin A, Tao L, Bast RC Jr, Zhang X.** Effective therapy of metastatic ovarian cancer with an oncolytic herpes simplex virus incorporating two membrane fusion mechanisms. Clin Cancer Res 2003; **9**: 2727–33.

21. **Barber GN.** Vesicular stomatitis virus as an oncolytic vector. Viral Immunol 2004; **17**: 516–27.

22. **Gadaleta P, Vacotto M, Coulombie F.** Vesicular stomatitis virus induces apoptosis at early stages in the viral cycle and does not depend on virus replication. Virus Res 2002; **86**: 87–92.

23. **Hobbs JA, Hommel-Berrey G, Brahmi Z.** Requirement of caspase-3 for efficient apoptosis induction and caspase-7 activation but not viral replication or cell rounding in cells infected with vesicularstomatitis virus. Hum Immunol 2003; **64**: 82–92.

24. **Kopecky SA, Willingham MC, Lyles DS.** Matrix protein and another viral component contribute to induction of apoptosis in cells infected with vesicular stomatitis virus. J Virol 2001; **75**: 12169–81.

25. **Janeway CA Jr.** Presidential Address to The American Association of Immunologists. The road less traveled by: the role of innate immunity in the adaptive immune response. J Immunol 1998; **161**: 539–44.

26. **Balachandran S, GN Barber.** Vesicular stomatitis virus therapy of tumors. IUBMB Life 2000; **50**: 135–8.

27. **Balachandran S, Porosnicu M, Barber GN.** Oncolytic activity of vesicular stomatitis virus is effective against tumors exhibiting aberrant p53, Ras, or Myc function and involves the induction of apoptosis. J Virol 2001; **75**: 3474–9.

28. **Marcus PI, Sekellick MJ.** Cell killing by viruses. II. Cell killing by vesicular stomatitis virus: a requirement for virion-derived transcription. Virology 1975; **63**: 176–90.

29. **Marvaldi JL, Lucas-Lenard J, Sekellick MJ, Marcus PI. Marcus.** Cell killing by viruses. IV. Cell killing and protein synthesis inhibition by vesicular stomatitis virus require the same gene functions. Virology 1977; **79**: 267–80.

30. **Ebert O, Shinozaki K, Huang TG, Savontaus MJ, Garcia-Sastre A, Woo SL.** Oncolytic vesicular stomatitis virus for treatment of orthotopic hepatocellular carcinoma in immune-competent rats. Cancer Res 2003; **63**: 3605–11.

31. **Kramm CM, Chase M, Herrlinger U, Jacobs A, Pechan PA, Rainov NG, Sena Esteves M, Aghi M, Barnett FH, Chiocca EA, Breakefield XO.** Therapeutic efficiency and safety of a second-generation replication-conditional HSV1 vector for brain tumor gene therapy. Hum Gene Ther 1997; **8**: 2057–68.

32. **Kovtun YV, Audette CA, Ye Y, Xie H, Ruberti MF, Phinney SJ, Leece BA, Chittenden T, Blattler WA, Goldmacher VS.** Antibody-drug conjugates designed to eradicate tumors with homogeneous and heterogeneous expression of the target antigen. Cancer Res 2006; **66**: 3214–21.

33. **Suzuki M, Tsuruoka C.** Heavy charged particles produce a bystander effect via cell-cell junctions. Biol Sci Space 2004; **18**: 241–6.

34. **Ikeda K, Ichikawa T, Wakimoto H, Silver JS, Deisboeck TS, Finkelstein D, Harsh GR 4th, Louis DN, Bartus RT, Hochberg FH, Chiocca EA.** Oncolytic virus therapy of multiple tumors in the brain requires suppression of innate and elicited antiviral responses. Nat Med 1999; **5**: 881–7.

35. **McCormick F.** Future prospects for oncolytic therapy. Oncogene 2005; **24**: 7817–9.

36. **Ball LA, Pringle CR, Flanagan B, Perepelitsa VP, Wertz GW.** Phenotypic consequences of rearranging the P, M, and G genes of vesicular stomatitis virus. J Virol 1999; **73**: 4705–12.

37. **Bishop DH, Repik P, Obijeski JF, Moore NF, Wagner RR.** Restitution of infectivity to spikeless vesicular stomatitis virus by solubilized viral components. J Virol 1975; **16**: 75–84.

38. **Zakowski JJ, Wagner RR.** Localization of membrane-associated proteins in vesicular stomatitis virus by use of hydrophobic membrane probes and cross-linking reagents. J Virol 1980; **36**: 93–102.

39. **Kopecky SA, Lyles DS.** The cell-rounding activity of the vesicular stomatitis virus matrix protein is due to the induction of cell death. J Virol 2003; **77**: 5524–8.

40. **Maher EA, Furnari FB, Bachoo RM, Rowitch DH, Louis DN, Cavenee WK, DePinho RA.** Malignant glioma: genetics and biology of a grave matter. Genes Dev 2001; **15**: 1311–33.

41. **Saito R, Bringas JR, McKnight TR, Wendland MF, Mamot C, Drummond DC, Kirpotin DB, Park JW, Berger MS, Bankiewicz KS.** Distribution of liposomes into brain and rat brain tumor models by convection-enhanced delivery monitored with magnetic resonance imaging. Cancer Res 2004; **64**: 2572–9.

42. **Zhang T, Matsumura A, Yamamoto T, Yoshida F, Nose T, Shimojo N.** Comparison of gadobenate dimeglumine and gadopentetate dimeglumine: a study of MR imaging and inductively coupled plasma atomic emission spectroscopy in rat brain tumors. AJNR Am J Neuroradiol 2002; **23**: 15–8.

43. **Machein MR, Knedla A, Knoth R, Wagner S, Neuschl E, Plate KH.** Angiopoietin-1 promotes tumor angiogenesis in a rat glioma model. Am J Pathol 2004; **165**: 1557–70.

44. **Balachandran S, Roberts PC, Kipperman T, Bhalla KN, Compans RW, Archer DR, Barber GN.** Alpha/beta interferons potentiate virus-induced apoptosis through activation of the FADD/caspase 8 death signaling pathway. J Virol 2000; **74**: 1513–23.

45. **Folkman J.** Angiogenesis in cancer, vascular, rheumatoid and other disease. Nat Med 1995; **1**: 27–31.

46. **Boehm T, Folkman J, Browder T, O'Reilly MS.** Antiangiogenic therapy of experimental cancer does not induce acquired drug resistance. Nature 1997; **390**: 404–7.

47. **King GD, Curtin JF, Candolfi M, Kroeger K, Lowenstein PR, Castro MG.** Gene therapy and targeted toxins for glioma. Curr Gene Ther 2005; **5**: 535–57.

48. **Han J, Yang L, Puri RK.** Analysis of target genes induced by IL-13 cytotoxin in human glioblastoma cells. J Neurooncol 2005; **72**: 35–46.

49. **Westphal M, Ram Z, Riddle V, Hilt D, Bortey E.** Gliadel wafer in initial surgery for malignant glioma: long-term follow-up of a multicenter controlled trial. Acta Neurochir (Wien) 2006; **148**: 269–75.

ПЛАЗМИДЫ, КОДИРУЮЩИЕ МАТРИКСНЫЙ ПРОТЕИН ВИРУСА ВЕЗИКУЛЯРНОГО СТОМАТИТА В КАЧЕСТВЕ ПРОТИВООПУХОЛЕВОГО АГЕНТА, ИНГИБИРУЮЩЕГО РОСТ ГЛИОМЫ КРЫС *IN SITU*

Цель: **изучить способность матриксного протеина (М протеина) вируса везикулярного стоматита (ВВС) угнетать рост глиомы *in situ*. *Материалы и методы:* сконструирована рекомбинантная плазмида, кодирующая М протеин ВВС, которая затем была трансфецирована в культивированные клетки глиомы С6 *in vitro*. Клетки глиомы С6, трансфецированные инкапсулированным в липосомы М протеином (ЛИМП), имплантировали интракраниально для изучения туморогенности. В эксперименте крысам с трансплантированной интракраниально глиомой С6 (исходный штамм) внутривенно вводили ЛИМП. Апоптотическое действие М протеина на опухолевые клетки изучали с применением флуоресценцентной микроскопии (окрашивание по Хехсту), проточной цитометрии (окрашивание пропидиумом йодидом), TUNEL; васкуляризацию опухоли оценивали гистологически и иммуногистохимически с применением анти-CD31 моноклональных антител. *Результаты:* М протеин может индуцировать лизис клеток глиомы *in vitro*. Ни у одного животного с трансплантированными клетками глиомы, обработанными ЛИМП, не возникали опухоли значительного размера, тогда как у всех крыс из контрольной группы опухоли развивались. В группе животных, которым вводили ЛИМП, опухоли были меньшего объема и отмечали увеличение продолжительности жизни животных. Показано, что М протеин проявляет антиангиогенные свойства и обладает способностью индуцировать апоптоз. *Выводы:* М протеин ВВС ингибирует рост глиомы *in vitro* и *in situ*. На этой основе может быть разработана потенциально новая биотерапевтическая стратегия для лечения пациентов с глиомами.**

Ключевые слова: **генная терапия, глиома, липосомы, матриксный протеин, плазмиды, туморогенность, вирус везикулярного стоматита.**